Mutation of the proline P81 into a serine modifies the tumour suppressor function of the von Hippel-Lindau gene in the ccRCC

Franck Chesnel, Emmanuelle Jullion, Olivier Delalande, Anne Couturier, Adrien Alusse, Xavier Le Goff, Marion Lenglet, Betty Gardie, Caroline Abadie, Yannick Arlot-Bonnemains

Mutation of the Proline P81 into a Serine modifies the tumor suppressor function of the von Hippel-Lindau gene in the ccRCC.

Franck Chesnel [1]., Emmanuelle Jullion [1]., Olivier Delalande [1]., Anne Couturier [1]., Adrien Alusse [1]., Xavier Le Goff [1]., Marion Lenglet [2, 3]., Betty Gardie [2, 3]., Caroline Abadie [4] . Yannick Arlot-Bonnemains [1*] .

1- CNRS UMR6290- Université Rennes 1 -SFR-UMSCNRS 3480-INSERM 018- 2 ave du Pr L Bernard-35042-Rennes-Cedex
2- Ecole Pratique des Hautes Etudes, EPHE, Université Paris Sciences et Lettres -
3- Nantes Université, CNRS, INSERM, l'institut du thorax, F-44000 Nantes, Nantes
4- Institut de cancérologie -boulevard Jacques Monod-44805-Saint Herblain Cedex

***Corresponding author**

Yannick Arlot-Bonnemains -

CNRS UMR6290- Université Rennes 1

2 ave du Pr L Bernard-35042-Rennes-France

Tel :33(0)223234696

Fax: 33(0)223234478

N° orcid : 0000-0003-4633-5650

Chesnel : franck.chesnel@univ-rennes1.fr- **N° orcid** : 0000-0002-1384-4056
Jullion : emmanuelle.jullion@univ-rennes1.fr
Delalande: olivier.delalande@univ-rennes1.fr
Couturier : anne2bzh@orange.fr
Alusse : adrien.alusse@univ-rennes1.fr
Le Goff : xavier.le-goff@univ-rennes1.fr **N° orcid** : 0000-0002-5297-2421
Lenglet : marion.lenglet@univ-nantes.fr
Gardie : betty.gardie@univ-nantes.fr **N° orcid** : 0000-0002-8206-8329
Abadie : Caroline.Abadie@ico.unicancer.fr
Arlot-Bonnemains : yannick.arlot@univ-rennes1.fr

Abstract

Background: The von Hippel Lindau disease is an autosomal dominant syndrome associated with tumor formation in various tissues such as retina, central nervous system, kidney, adrenal glands. VHL gene deletion or mutations support the development of various cancers. Unclassified VHL variants also referred as "of unknown significance" result from gene mutations that have an unknown or unclear effect on protein functions. The P81S mutation has been linked to low penetrance Type 1 disease but its pathogenic function was not clearly determined. **Methods**: We established a stable cell line expressing the $pVHL_{213}$ (c.241C>T, P81S) mutant. Using biochemical and physiological approaches, we herein analyzed pVHL folding, stability and function in the context of this VHL single missense mutation. **Results:** The P81S mutation mostly affects the non-canonical function of the pVHL protein. The cells expressing the $pVHL_{213}$P81S acquire invasive properties in relation with modified architecture network.

Conclusion: We demonstrated the pathogenic role of this mutation in tumor development in *vhl* patients and confirm a medical follow up of family carrying the c.241C>T, P81S.

Introduction

The von Hippel Lindau (VHL) gene is a tumor suppressor gene which deletion or invalidation by mutations induce multiple tumors including renal and central nervous system hemangioblastoma, (CNS), clear cell carcinoma (ccRCC) and pheochromocytoma. The most studied well-known function of pVHL is to be a substrate recognition component of an E3 ubiquitin ligase complex comprising Elongin B/Elongin C, Cullin 2 and Rbx1 [1] to regulate the hypoxia-inducible-factors (HIF-α) transcription factors. The association of pVHL to HIF-1α and HIF-2α is oxygen-dependent and triggered through hydroxylation of HIF [2] ; it results in ubiquitination and proteasome-dependent degradation of HIF-α.

Based on the pathologies, VHL disease is classified in two distinct types, Type 1 and Type 2, depending on the development of pheochromocytoma (Type 2) or not (Type1). Type 1 subtype describes typical phenotype VHL manifestation as hemangioblastoma and RCC. Type 2 is subdivided into three subtypes: patients with Type 2A and B develop pheochromocytomas and other VHL manifestations, with a low risk (Type 2A) or high risk (Type 2B) of RCC, patients with Type 2C develop only pheochromocytomas. Patients with ccRCC (kidney tumor of epithelial origin) are therefore mostly classified into Type 1 and 2B [3]. Finally, a third class of patients (Type 3) is characterized by the development of erythrocytosis, the most described being the Chuvash polycythemia associated with the homozygous *VHL*-R200W mutation [4][5]. At the molecular level, Type 1 families are characterized with various mutations (missense, frameshift, nonsense, splice) as well as in frame deletion/insertions or partial/complete deletions of *VHL* gene, leading to a loss of pVHL function and the development of a large spectrum of cancerous tumors [3]. On the other hand, VHL Type 2 families were mainly characterized by missense mutations (83.5%), with a low percentage of nonsense, frameshift, splice, in-frame deletion/insertions, or partial deletions.

With the exception of deletions which account for 30–40% of cases, most mutations cluster within two regions of high functional importance in pVHL protein, the Elongin C (amino acid residues 157-171) and HIF-α (amino acid (a.a) residues 91-113) binding domains which are highly evolutionarily conserved sequences [6]. Missense mutations could be deleterious for the protein leading to its functional inactivation and resulting in HIF-α accumulation and the expression of HIF target genes involved in signal transduction pathways responsible of hyperproliferation and/or tumorization.

Structurally, the pVHL protein consists of two functional protein binding domains, the β-domain (comprised of residues 63–155 and 193–204) and the α-domain (residues 155–193).

When analyzing the 3D structure of pVHL, three distinct pVHL interaction interfaces have been described engaging in exclusive interactions [7]. The α domain binds elongins and Cullin2 while the β sheet domain of pVHL extending from residues 63 to 157 binds and participates to the polyubiquitination and ultimately targets HIF-α for proteasomal degradation [8].

Among the 1230 mutations listed in the VHL database (http://umd.be/VHL) some mutants still remain biochemically uncharacterized [3]. Referred families diagnosed with P81S mutation linked to low penetrance Type 1 von Hippel-Lindau disease and a mild phenotype [9] [10]. A previous study investigating defects Type 2C associated mutant protein demonstrated at the molecular level the deleterious role involvement of $pVHL^{L188V}$, $pVHL^{P81S/L188V}$, $pVHL^{V84L.}$ [11].

In this study, we were interested in a family with two members who showed clinical symptoms of VHL disease. One member (III.2) developed a ccRCC at the age of 37. The genetic analysis has revealed the presence of c.241C>T (P81S) germline mutation. The genetic study of the progeny evidenced the presence of this same mutation in children (IV.4,5).

The use of *in silico* algorithms (HOPE, Symphony) indicated a possible pathogenicity of P81S mutation but not the GVGD that assigned a low genetic risk. [10]. Most of the analysis of the effect of the P81S mutations, were performed in relation with an additional mutation in the gene or exposure to trichlorethylene [12]. Most carriers with the only P81S mutation have no VHL-related manifestations [13] . The clinical observations made for the above family raised the need to understand the involvement of the mutation P81S in the development of VHL pathologies. We have undertaken a structural, biochemical and cellular study to characterize the pathogenicity of this mutation and to conduct a medical follow-up for practitioners.

Materials and methods

Site directed mutagenesis and plasmid construction

The plasmids pcDNA3.1-P_{PGK}-FlagHA-VHL_{213} and -VHL_{213} P81S were generated as follows : The ORF of VHL variant 1 (excised from pCMV2c-VHL_{213}, a generous gift from Dr A. Buchberger, Würzburg, Germany) was subcloned in pcDNA3.1-FlagHA (a kind gift from Dr S. Rouquier, Toulouse, France) with murine phosphoglycerate kinase (PGK) promoter [14]. P81S point mutation was introduced into the *VHL cDNA* inserted in pcDNA3.1-P_{PGK}-FlagHA-VHL_{213} using a sequential two-step PCR approach with the high-fidelity PCR master polymerase (Sigma Aldrich, St Quentin-Fallavier, France). The oligonucleotides used to carry out the site-directed mutagenesis were as follows: P81Sfor, 5'-TGC AAT CGC AGT TCG CGC GTC-3'; P81Srev, 5'- GAC GCG CGA ACT GCG ATT GCA-3'. The resulting final amplicon was cut with BamHI and XhoI (Promega, Charbonnière les bains, France) and inserted into empty pcDNA3.1-P_{PGK}-FlagHA (first linearized with the same restriction enzymes) with T4 DNA ligase (Promega).

All constructs were confirmed by Sanger sequencing, amplified in NEB5alpha bacteria (New England Biolabs, Evry, France) and purified using the Nucleobond Endofree plasmid purification kit (Macherey Nagel, Hoerdt, France) before transfection in mammalian cells.

Cell culture and transfections

The 786-O kidney cancer cell line, from the ATCC (LGC Standards), was cultured in RPMI-1640 (Life Technologies, Courtaboeuf, France) supplemented with 10% fetal calf serum and 1% penicillin/streptomycin at 37°C with 5% CO_2. Stable cell lines were generated by transfecting 786-O cells with pcDNA3.1-P_{PGK}-Flag-HA-VHL_{213}P81S using Avalanche-Omni (EZ-Biosystems, College Park, USA) and selected with 500µg/ml G418 (Life Technologies). The 786-O cells with pcDNA3.1-P_{PGK}-Flag-HA-VHL_{213}wt have been previously generated in the laboratory [14].

Protein extraction and immunoblotting

Cells were lysed in RIPA extraction buffer, or directly in Laemmli loading buffer. Equal amounts of proteins were separated by SDS-PAGE and transferred to nitrocellulose. Membranes were probed with antibodies against VHL (1:1,000; clone JD1956 [15]), HA (1:4,000; Roche), Flag (1:2,000; Sigma-Aldrich), β-tubulin (1:2,000; Sigma-Aldrich), cyclin D1 (1:500; Cell Signaling Technology), cullin-2 (1:450; Life Technologies), Elongin-C (1:1,000; Bio Legend), HIF2-α (1:500; Novus Biologicals). Immune complexes were detected as previously described [15].

Reporter assays

The parental 786-O or the stable 786-O-pVHL$_{213}$ and 786-O-pVHL$_{213}$-P81S cell lines were transfected with plasmids encoding Firefly-luciferase under the control of Hypoxia-Response-Elements (HRE-luciferase), and Renilla-luciferase for normalization. After a 24-h culture, luciferase activity was measured using a Dual-Luciferase®Reporter Assay System (Promega).

Wound healing assay

Cells were cultured at 37°C in a humidified atmosphere containing 5% CO_2 until confluence in culture-inserts 2 wells (Ibidi-Cell in focus; Clinisciences, Nanterre, France). Cells were treated or not with 10µg/ml mitomycin C (Sigma-Aldrich). Cell migration was then recorded every 15 min for 24 hours using an Axiovert 200M microscope equipped with a LD Plan-Neofluar 20×/0.4 Ph2 lens and an AxioCam MRm camera under the control of the ZEN 2012 software (Zeiss). The wound area was measured using the Simple PCI6 software (Hamamatsu Photonics, Massy, France). The analysis of cell migration during the assay was performed with the MRI Wound Healing Tool (http://dev.mri.cnrs.fr/projects/imagej-macros/wiki/Wound_Healing_Tool) using Image J software.

Spheroid formation

Five thousand cells were plated in medium per well of a 96-well plate with round bottom previously coated with Poly(2-hydroxyethyl-metacrylate) (Sigma-Aldrich) and incubated for up to 4 days to allow spheroid formation. The spheroids were analyzed by microscopy (DMIRB- Leica) and the size calculated using Image J software.

Invasion tumor assay on Matrigel

The spheroids were embedded in a gel composed of a mixture of Matrigel (2mg/ml; Corning) in full medium RPMI-1640 supplemented with 10% fetal calf serum and 1% penicillin/streptomycin at 37°C with 5% CO_2. Cell migration away from the spheroids was recorded under a video microscope (Delta vision-MRIC-SFR-UMS-CNRS 3480-INSERM018) for several hours.

Modeling

The pVHL$_{213}$ model is derived from the protein databank structure PDB ID:1VCB completed by the i-tasser server (https://zhanglab.ccmb.med.umich.edu/I-TASSER/).

Results

Clinical evaluation

The family A with members suffering from VHL disease studied in the present study was recruited in the PREDIR center (France). A clear cell Renal Cell Carcinoma (ccRCC) was diagnosed in the proband (III.2) at the age of 37 and treated with radical nephrectomy. Genetic analysis revealed the germline missense mutation c.241C>T, p.Pro81Ser (P81S) in the *VHL* gene (Reference sequence: NM_000551). A retrospective study of the potential presence of mutation in parents and descendants was undertaken. There were originally three patients with the P81S mutation in the *VHL* gene (II.8. Genetic testing of the descendants identified the P81S mutation in the genome of the two 8- and 13-years-old children. In addition, sequencing of the *VHL* gene of members of the background family showed the presence of the mutation for the sister of and the father who are respectively 65 and 38 years old (Fig.1 II.1, III.1). Besides the proband's ccRCC, none of the carriers displayed any other signs of VHL-related manifestations including the 65-year-old father. The variant was identified in the index case and was declared as pathogenic. The hypothesis is that in the case of a spectrum tumour in a person carrying a VHL variant, the portal of entry here being renal, there is probably a loss of the 3p on the wild-type allele. Tumor material was not available to perform the analysis. Surveillance program, according to the French VHL guidelines (Centre PREDIR) (including Magnetic Resonance Imaging (MRI) of the Central Nervous System, MRI or Ultrasound of the Abdomen, ophthalmological examination, measurement of urinary metanephrines), was normal for all of the carriers. The single manifestation in the proband and the absence of clinical signs in the other mutation carriers questioned about the penetrance of the P81S germline mutation.

Structural evaluation of the P81S mutation

The *VHL* tumor suppressor gene encodes a protein which contains two main structural domains÷ (β domain a.a 65-154 and α–domain- a.a157-193) held together by two linkers and a polar interface. (Fig. 2A). Previous studies combining structural information and computational analysis have distinguished three distinct interfaces [6]**,** each interface refined motifs involved in specific protein-protein interactions. Moreover, five distinct pVHL interaction interfaces (A, B, C, D and E, Fig. 2A) are engaged in exclusive interactions with different interactors and may partially explain the pVHL binding plasticity. Interface A (a.a 154-189) is important for VCB complex formation and interface B (a.a 60-103) forms the HIF-1α binding-site while interface C (a.a 157-190) participates in the Cullin2 interaction.

The proline 81 is located in the β-domain and included in a turn in the molecular structure (between the β strands #1and #2**,** Fig. 2, B and C). As many other proline residues of pVHL, Pro81 defin**es** boundaries of secondary structure elements such as the β strands and could be essential for ternary structure formation (Fig. 2B).

Due to its localization, the P81S substitution might cause significant structural perturbations in the β domain organization [7]. Nevertheless, the reported link of the P81S substitution to Type 1 VHL disease remains enigmatic, given the lack of significant functional defects of the pVHL-P81S mutant protein *in vivo* [13]. Such altered pVHL may still be able to exert some of its functions and/or may gain novel ones. Structural analyses suggest a modification of the β domain, but biochemical studies are required to clarify the alterations in biological functions.

Biochemical impact of P81S mutation on pVHL$_{213}$ function(s)

To analyze the potential effect(s) of the mutation P81S on the function of pVHL, the Proline in position 81 was mutated into the polar uncharged amino acid, Serine. We stably transfected the renal carcinoma cell line 786-O (VHL-/-) which does not express wild-type *VHL* with the plasmid pcDNA3.1-P_{PGK}-Flag-HA-VHL$_{213}$P81S to moderately express the pVHL protein with the mutation of interest. Three positive clones (namely E1, E6, and C7) were obtained and controlled for mutation by sequencing. The expression level of the protein pVHL was then analyzed in the different cell lines: parental 786-O, 786-O-pVHL$_{213}$ (wild type) and the three clones corresponding to 786-O-pVHL$_{213}$-P81S. The immune detection revealed a positive expression of the VHL protein in the three clones (Fig. 3A).

Loss of pVHL activity might be the result of pVHL functional inactivation or degradation that is often observed in Type 1 pVHL mutants. We thus addressed the question whether the prediction of the stability of pVHL mutants may influence its functionality. As all clones obtained after selection expressed identical levels of the protein (Fig. 3A), we selected one of the three clones (E6). Tubulin visualization shown no obvious architectural differences were discriminant for the three cell lines (Sup Fig.1). In order to control the stability of the mutant pVHL$_{213}$-P81S protein, the different stable cell lines were treated with the protein synthesis inhibitor cycloheximide (CHX) for 3 and 7 hours. CyclinD1 expression confirmed the CHX treatment efficiency. Expression levels of pVHL in the 786-O-pVHL$_{213}$-P81S stable cell line compared to that of wild type pVHL in the 786-O-pVHL$_{213}$ were measured by immunoblotting (Fig. 3B and C). The stability of the pVHL$_{213}$-P81S was not significantly changed. Indeed, evaluation of the amount of the pVHL$_{213}$-P81S and pVHL$_{213}$ showed that in both cases the

236 remaining amounts of proteins after a 7-hour treatment with CHX consist in respectively 56%
237 and 66% of the initial amount of endogenous protein (Fig. 3C, p=0, 396).
238 The pVHL tumor suppressor functions as a redox sensor, which controls stability of the
239 hypoxia-inducible transcription factor family (HIFs) amongst other proteins.
240 The VHL gene product is the substrate recognition subunit of a multiprotein E3 ubiquitin ligase
241 complex, in association with the scaffold protein Cul2, the ring box protein Rbx1 and the
242 adaptor proteins, Elongins B and C. As most VHL mutations affect the oxygen-dependent
243 regulation of HIF2-α cellular levels, we tested whether the mutant $pVHL_{213}$-P81S participated
244 to the E3 ligase complex to ubiquitinate and ultimately lead to HIF2-α degradation. In order to
245 prevent HIF2-α proteasomal degradation that rapidly occurs upon polyubiquitination by pVHL
246 and therefore allow its co-immunoprecipitation, the cells were first treated with the proteasome
247 inhibitor (MG132) up to 5 hours before harvest and the proteasome inhibitor efficacy in
248 preventing HIF2-α degradation was verified by western blotting (Fig. 4A).
249 Immunoprecipitation of flagged proteins expressed in 786-O-$pVHL_{213}$ and 786-O-$pVHL_{213}$-
250 P81S was then performed. As observed on Fig. 4B, Cullin 2 was similarly co-precipitated by
251 both $pVHL_{213}$ and $pVHL_{213}$-P81S proteins. Likewise, HIF2-α which associated with the
252 $pVHL_{213}$ was also detected with the immunoprecipitated $pVHL_{213}$-P81S (Fig. 4B). The ratio
253 HIF2-α/pVHL and Cul2/VHL evaluated on three distinct experiments revealed that HIF2-
254 α/pVHL ratio appears stronger in the 786-O-$pVHL_{213}$-P81S than in the 786-O-$pVHL_{213}$ cells
255 but only after 2 hours (Fig. 4C p= 0,0313) and 5 hours (Fig. 4C p= 0,0041) of treatment with
256 MG132 (n=5-Fig. 4C). This ratio is not significantly different in non-treated cells. (Fig 4C).
257 The amount of Cul2 immunoprecipitated with the 786-O-$pVHL_{213}$-P81S did not change notably
258 from the amount of Cul2 detected in the 786-O-$pVHL_{213}$. These first results show that the P81S
259 mutation does neither diminished recruitment of E3-ligase subunit such as Cullin2 nor the
260 binding of the major substrate HIF-2α.
261 We then evaluated the amount of HIF2-α in the different cell lines incubated in the presence of
262 protein synthesis inhibitor (CHX) (Fig. 3B). In the absence of CHX treatment (t=0), the amount
263 of HIF2-α was significantly diminished in the 786-O-$pVHL_{213}$ cells as well as in 786-O-
264 $pVHL_{213}$-P81S cells, compared to the level detected in 786-O cell lines (*p value = 0.00173 and*
265 *0.04156, respectively)* (Fig. 3D). No difference in HIF2-α level was observed between 786-O-
266 $pVHL_{213}$ and 786-O-$pVHL_{213}$ P81S cells (*pvalue* : 0.685) (Fig. 3 B and D). After treatment with
267 CHX, the quantity of HIF2-α remaining in the $pVHL_{213}$ and $pVHL_{213}$-P81S cells represented
268 39% of the initial amount of the HIF2-α evaluated in the 786-O cells (Fig. 3D). The level of

immunodetected HIF2-α associated to pVHL did not seem to change in 786-O $pVHL_{213}$-P81S cells as well as in 786-O $pVHL_{213}$ (Fig. 3D).

To go further in understanding the role of the mutation towards the canonical function of pVHL, we also compared the amounts of the protein HIF2-α in the 786-O, 786-O-$pVHL_{213}$ and 786-O-$pVHL_{213}$-P81S cell lines under normoxia *versus* chemical hypoxia condition (19 hours of $CoCl_2$ treatment). Under normoxic conditions, HIF2-α was lower in 786-O-$pVHL_{213}$ cells (t-test, p=0.02616) as well as in 786-O-$pVHL_{213}$-P81S cells (t-test, p=0.004998) in comparison to 786-0 (Fig. 3E and F) . After treatment of the cells with $CoCl_2$ for 19h, the quantity of immuno detected HIF2-α increased in both $pVHL_{213}$ cells and $pVHL_{213}$-P81S cell lines. In the presence of $CoCL_2$, significant modification of HIF2-α amount was observed between 786-O cells and 786-O-$pVHL_{213}$ (t-test, p=0.0365) and 786-O-$pVHL_{213}$-P81S cells (t-test, p=0.0194). In contrast, no significant variation of HIF2-α was observed between when 786-O-$pVHL_{213}$ and 786-O-$pVHL_{213}$-P81S after hypoxic treatment (Fig. 3F).

To better understand the effect of the mutation P81S on the regulation of HIF, a functional study was performed using a Hypoxia Response Elements (HRE) dependent reporter assay [5] (Fig. 4D). The ability of $pVHL_{213}$ and mutant $pVHL_{213}$-P81S to downregulate firefly luciferase activity (reflecting HIF activity) was tested in 786-O cells and the results confirmed that $pVHL_{213}$ as well as $pVHL_{213}$-P81S displayed a similar luciferase activity, largely reduced compared to that in 786-O cells (Fig. 4D).

Altogether, our data show that the formation of the E3 ligase complex is not fundamentally altered when $pVHL_{213}$ is mutated on Pro 81(to Ser) and the modest variations in HIF2-α (binding and stability) observed in the presence of $pVHL_{213}$-P81S cannot account for the development of the pathology in a member of the family.

The P81S Mutation of $pVHL_{213}$ modifies migration properties of renal cells

Dysregulation of the *VHL* gene is closely associated with ccRCC. Other pVHL, HIF-independent, functions have been shown to be required and help to explain why loss of pVHL leads to renal cancer. How the P81S mutation of pVHL might explain the development of the ccRCC for a 37-year-old patient in a HIF-independent manner was thereafter investigated. As malignant cancer cells exploit their intrinsic migratory ability to invade adjacent tissues and the vasculature, we have studied cell morphology and dynamics. Transformed cells often exhibit different growth characteristics than non-transformed cells. Therefore, in a first round of experiments, we investigated the migration/invasion properties of these different cell lines. First, we set up a standard scratch wound healing assay (Fig. 5A). The migration of cells in the

specific wound area was recorded every 15 min during 16 hours (= 1000 minutes), *i.e.* until the scratch area was fully repopulated by all of the tested cell lines (Fig. 5A). The images from the beginning to the end of a 16 hours incubation period were captured. The end of recording time was determined at 16h when the slowest moving cells (786-O-pVHL$_{213}$ cells - dark line) were just about to fully fill in the scratch (Fig. 5B). The 786-O cells, which do not express wild type pVHL, covered the wound caesura after 7.5 hours (Fig. 5B, grey line) whereas the 786-O pVHL$_{213}$-P81S stably transfected cells close the caesura in 6 hours (Fig. 5B, dotted line). Therefore, comparison of the cells stably transfected with the pcDNA-VHL$_{213}$ and those transfected with the pcDNA-VHL$_{213}$-P81S showed modification of cell migration when *VHL* is mutated. The time-dependent changes of the open area due to cell migration were scored for each cell type as the time to repopulate 50% of the gap. The parental 786-O cells invaded 50% of the area after 202,9 ± 13,7 min versus 368 ± 48 min for 786-O pVHL$_{213}$ (Fig. 5C) The 786-O cells expressing pVHL$_{213}$-P81S covered 50% of the caesura in 162,4 ± 11 min. The statistical analysis of the experiments for each cell line revealed a significant difference in time of migration between 786-O and 786-O-pVHL$_{213}$ (n=8 *p .value 0.0006333 t test*) and between 786-O-pVHL$_{213}$ and 786-O-pVHL$_{213}$-P81S (n=7 *pvalue 0.0003016 - t-test*) (Fig.5C). A slight difference of migration was observed when comparing the migration of between the 786-O and 786-O-pVHL$_{213}$-P81S (n=6 *pvalue : p 0,01342 - t test*)(Fig.5C).

Impact of pVHL$_{213}$-P81S on aggregation properties of the transfected tumoral cells

Multicellular aggregates of cells and tumor organoids have become preclinical model systems of great interest for studying tumor behaviors. Spheroids more faithfully reproduced the tumor macrostructure compared to classical 2D monolayers. As previously demonstrated, the spheroid formation assay was performed to determine the properties of 786-O cells to aggregate and the impact of wild type and mutated pVHL on this cell aggregation. The three cell lines 786-O, 786-O-pVHL$_{213}$ and 786-O-pVHL$_{213}$-P81S were tested for spheroid formation (Fig. 6A) and the expression of pVHL was controlled in the cell lines (Fig 6B). As previously shown, the 786-O cell line formed multicellular spheroids with highly uniformity in size and cell density[14]. Interestingly the 786-O-pVHL$_{213}$-P81S cells formed a cluster of cells which structure differed from the structures observed with either the 786-O cells or the 786-O-pVHL$_{213}$ cells. The contour of spheroids appeared as an intermediate shape between the one observed when prepared with the 786-O cells and the 786-O-pVHL$_{213}$-P81S with dense cell-cell interactions and borders slightly widespread (Fig. 6A).

The ability of cells to grow in a semi-solid medium was further recorded while testing the characteristics of malignantly transformed cells. The morphology of the spheroids obtained

with the 786-O cells was not changed when they were embedded in the Matrigel for 24 hours. The appearance of the 786-O-pVHL$_{213}$ aggregates deposited in the Matrigel was transformed and became more compact (Fig. 5C). In contrast, the 786-O-pVHL$_{213}$-P81S spheroids appeared modified, the inner part of the spheroid became dense and compact whereas the peripheral cells escaped from the spheroids and migrated into the Matrigel (Fig. 6C). These observations strongly suggest that 786-O cells acquire invasive features upon expression of pVHL$_{213}$-P81S. The different 786-O-pVHL$_{213}$-P81S clones obtained in our study showed identical behavior with respect to spheroid formation and migration into Matrigel (Sup Fig 2).

The actin cytoskeleton undergoes dynamic assembly and disassembly during cell crawling, which regulates protrusion formation, focal adhesion assembly/disassembly, and contractile filament organization. Assembly of the actin cytoskeleton is essential for invasion and cell migration. Cell migration requires the formation of various structures, such as invadopodia and pseudopodia, which require actin assembly that is regulated by specialized actin nucleation factors. Cell migration is the result of a multistep and complex process initiated by the transformation of the actin cytoskeleton. The length of filaments varies greatly, the filaments are cross-linked into imperfect bundles and networks. The disruption of the actin cytoskeleton inhibits cell migration and adhesion [16]. The orientation of F-actin fibers (parallel and random distribution) was analysed in the different cell lines used in this study. The F-actin network was organized as dense and parallel fibers along the long axis of the 786-O pVHL$_{213}$ cells while actin fibers were longer and less dense in 786-O cells (Fig. 6D). In contrast, actin fibers were very short and mostly located near the membrane in cells expressing pVHL with the P81S mutation (Fig 6D). In conclusion, the architectural network exhibited different organisation in the cells expressing or not pVHL$_{213}$ or pVHL$_{213}$-P81S.

Discussion

In this study, we described the workup of a family carrying a germline missense mutation c.241C>T, p.Pro81Ser (P81S) with carriers' members : a 37-year-old adult diagnosed with a ccRCC and some family members carrying the mutations who were asymptomatic. Moreover, the P81S in the *VHL* gene has been identified in 4 other French families in the PREDIR molecular genetics laboratories network (https://predir.org/View/accueil.aspx). One proband had a ccRCC at a young age (28 years), 3 others had pheochromocytoma or paraganglioma at older ages (68 and 70 years for two of them, age unspecified for the third case).

Other proline mutations have been reported in databases as well, including Proline in positions 2, 86, 97 and converted in non-polar residue (Leu, Ala), polar (Ser) or basic amino acid residues (Arg, His). Depending on the amino acid, the mutants were classified benign or as variants of uncertain significance (VUS). Patients bearing the Pro86Ala/Arg/Ser/His mutations and developing hemangioblastoma and kidney cysts were described as probably pathogenic [3][17].

The presence of the P81S mutation in various families were associated with low penetrance or mild phenotype together in the German VHL family with one affected member who developed central nervous system (CNS) hemangioblastoma and renal cell carcinoma as well as kidney and pancreatic cysts [3]. Moreover, the substitution of the Proline 97 by a Leucine was described as pathogenic when associated with another mutation Leu166Pro [18]. It was therefore of interest to discriminate the role of the mutant the P81S VHL pathology.

We employed a set of *in silico* predictions and *in cellulo* and *in vitro* methods along with structural analysis to investigate whether the single P81S mutation is involved in disease development or neutral.

Predictions for the impact of the P81S substitution in the *VHL* gene, obtained by *in silico* analysis, showed a discrepancy depending on the prediction tools. The different *in silico* algorithms used to analyze the mutants reported the difficulties to classify the P81S VHL mutation as it could come out as potentially pathogenic or as unclassified variant (www.umd.de). We should have replaced the Proline into an Alanine which is also a nonpolar and hydrophobic amino acid This modification brings great complexity to the structural and biochemical structure but it is consistent with the pathology. We are aware that serine not only changes the organization of the molecule in 3 dimensions and induces charge modifications that

can generate new bonds. We focused on the patient's mutation P81S despite the fact that it combines the change in charge and structure.

In particular, replacement of proline by serine at residue 81 might disturb the native pVHL structure by destroying a rigid link known to be associated with proline and to favor the formation of hydrogen bonds with neighboring polar amino acids. However, as many other proline residues of pVHL, Proline 81 plays a role in defining the boundaries of secondary structure elements such as the β-strands composing the core of the protein. Indeed, among the Proline residues, several are delimiting the extremities of a β strand: Pro71 and Pro81 (start and end of β1), Pro95 and Pro99 (start and end of β3), the Pro102 and Pro103 pair (start of β4) and Pro146 and Pro154 (start and end of β 7) (Fig. 2C). The distribution of many of these specific amino acids along the pVHL sequence allows the chaining of short β-strands and a succession of turns organizing the β domain of the protein. It should nevertheless be emphasized that the *in-silico* prediction can only give an approximation for pathogenicity that need to be validated by *in vitro* and in vivo experimental validation.

Most frequently reports showed that Type 1-associated pVHL mutant proteins are most frequently reported as failing to assemble the E3-ubiquitin ligase [11]. The risk relevance of this mutation was only identified in TCE-induced ccRCC or in association with other mutations [19] [11]. Moreover, previous studies have speculated that the impact of the P81S mutations might even be stronger in combination with the L188V mutation [13]. Altogether, both mutations likely influence protein-protein interactions. Previous reports on structural studies of the P81S variant mentioned that this proline to serine substitution was not expected to cause significant structural perturbations on its own, but it has been proposed to affect the orientation of the neighboring residue Arg82, whose side chain forms the center of a hydrogen bond network stabilizing both the α/β domain interface of pVHL-Elongin C [20].

The establishment of the stable cell line became essential to investigate the pathogenicity of $pVHL_{213}$-P81S. As mentioned in previous work, the absence of native conformation could highly lead to a destabilization of the protein [11][21]. In addition, the B domain is implicated in substrates' recognition like the hypoxia induced factors alpha (HIFs-α, the A interface is important for the formation of the VBC complex [7][22]. Because of the critical location of P81S within the β-sheet domain of pVHL, we inferred that protein binding, including HIF-2α, may be impaired. In our hands, the stability of the protein $pVHL_{213}$-P81S amount was not significantly different from that of wild type $pVHL_{213}$, suggesting that the P81S mutation does not trigger a total protein unfolding as often observed for type I pVHL mutation.

Moreover, the E3 complex was still formed with pVHL$_{213}$-P81S and able to bind HIF2-α. The amount of HIF2-α in cells expressing pVHL$_{213}$-P81S was detected mostly more related to the amount of the protein quantified in the 786-O cells. Therefore, the particular P81S mutation does not seem to abolish (or diminish) HIF binding, as one should expect with a type I mutation.

The role as hypoxia sensing component was conveniently used to explain some of the main VHL manifestations. However, it fails almost entirely in predicting the pathogenic risk of several mutations not directly connected with HIF-1α degradation. Defective HIF-1/2-α regulation is believed to be sufficient to induce development of hemangioblastomas and to be a key pathogenic event in the development of RCC but in the present study, the ability of pVHL$_{213}$ P81S to down-regulate HIF, at least in normoxic conditions, suggest that other pVHL-HIF-independent functions may be affected to explain the development of the ccRCC.

Lastly, the experimental results did not explain why in the family described in this study one member developed a ccRCC. These observations reveal a preferentially non-canonical function of pVHL$_{213}$-P81S. pVHL plays many roles, including a very important one in the formation of the extracellular matrix, epithelial differentiation and correct interaction between epithelial cells and the extracellular matrix [23]. Moreover, deletion of the *VHL* gene can activate β-catenin [an important mediator of EMT [24]. The inactivation of pVHL in pheochromocytoma has led to the up-regulation of seven genes, such as *CTGF, SDCBP, CYR61, COL3A1, COL1A1, COL5A2* and *SERPIN1*, which are closely related to cell proliferation, migration and differentiation [25].

This naturally led us to test, in migration 2D and invasion 3D assays, the hypothesis that P81S mutation of pVHL would impact cell migration and/or invasiveness int the 2D or 3D assays. We indeed observed a more migrating potency of the 786-O-pVHL$_{213}$-P81S. The speed of pVHL$_{213}$-P81S cell invasion, the shape and the size of the spheroids, as well as the behavior of the cells from the spheroids, when included in Matrigel, supported the modified function of pVHL when the P81S mutation is present.

Other Prolines (P86 and P97) located in the β-domain have been shown pathogenic when mutated, while inducing hemangioblastomas and ccRCC [26]. Also in the B-domain , the Ser 72 of pVHL when mutated into proline was described as pathogenic, associated with hemangioblastomas and pancreatic cyst [27][28]. Functional interaction of pVHL with AURKA was shown to modulate microtubules stability and dynamics. Mutations of the Ser into Pro participate in tumor initiation/progression [29]. In the present situation, the P81S mutation might induce structural transformations that could affect the functions of the

surrounding amino acids. This would therefore modify the non-canonical functions of the protein. The $pVHL_{213}$-P81S drive morphological cell changes that might be induced by expression of protein involved in cell adhesion and migration expression. Conclusively, our results demonstrate that the P81S mutation changes the cellular tumor suppressor function of pVHL213 and confers to the cells a migratory and invasive behavior. Moreover, combining MetaDome and Mobidetails [30][31] web server which help to interpret DNA variants in the context of molecular diagnosis, we observe that the P81S mutant is classified as intolerant and certainly pathogenic (Supp Fig. 3). The development of kidney cancer in young subjects in the family studied and the detection of pheochromocytomas and angioblastomas in patients (http://www.umd.be/) strongly suggests a medical follow-up in the members of the impacted families. Further investigations will be necessary to define in more details the molecular pathway involved in cell transformation with such pVHL mutant.

References

[1] Lewis MD, Roberts BJ Role of the C-terminal α-helical domain of the von Hippel–Lindau protein in its E3 ubiquitin ligase activity. Oncogene 2004; 23: 2315–2323.

[2] Maranchie JK, Vasselli JR, Riss J, Bonifacino JS, Linehan WM, Klausner RD The contribution of VHL substrate binding and HIF1-α to the phenotype of VHL loss in renal cell carcinoma. Cancer cell 2002; 1 : 247–255.

[3] Nordstrom-O'Brien M, van der Luijt RB, van Rooijen E, van den Ouweland AM, Majoor-Krakauer DF, Lolkema MP, *et al.* (2010) Genetic analysis of von Hippel-Lindau disease. Hum Mutat. 2010; 31 : (5) 521-537.

[4] Zbar B, Kishida T, Chen F, Schmidt L, Maher ER, Richards FM, *et al.* Germline mutations in the Von Hippel-Lindau disease (VHL) gene in families from North America, Europe, and Japan. Human Mutat. 1996; 8: 348–357.

[5] Lenglet M, Robriquet F, Schwarz K, Camps C, Couturier A, Hoogewijs D, *et al.* Identification of a new VHL exon and complex splicing alterations in familial erythrocytosis or von Hippel-Lindau disease. Blood 2018; 132: 469–483,

[6] Leonardi E, Murgia A, Tosatto SCE Adding structural information to the von Hippel-Lindau (VHL) tumor suppressor interaction network. FEBS Letters. 2009*;* 583 : 3704–3710.

[7] Minervini G, Quaglia F, Tabaro F, Tosatto SCE Genotype-phenotype relations of the von Hippel-Lindau tumor suppressor inferred from a large-scale analysis of disease mutations and interactors. PLoS Comput Biol. 2019; 15 : e1006478.

[8] Ivan M, Kaelin WG. The von Hippel–Lindau tumor suppressor protein. Current Opinion in Genetics & Development. 2001; 11: 27–34.

[9] Hes FJ. Cryptic von Hippel-Lindau disease: germline mutations in patients with haemangioblastoma only Journal of Medical Genetics. 2000; 37 939–943.

[10] Alosi D, Bisgaard M, Hemmingsen S, Krogh L, Mikkelsen H, Binderup M Management of Gene Variants of Unknown Significance: Analysis Method and Risk Assessment of the VHL Mutation p.P81S (c.241C>T). Current Gen. 2016*;* 18: 93–103,

[11] Knauth K, Cartwright E, Freund S, Bycroft M, Buchberger A. *VHL* Mutations Linked to Type 2C von Hippel-Lindau Disease Cause Extensive Structural Perturbations in pVHL. J Biol Chem. 2009; 284: 10514–10522.

[12] DeSimone MC, Rathmell WK, Threadgill DW. Pleiotropic Effects of the Trichloroethylene-Associated P81S VHL Mutation on Metabolism, Apoptosis, and

503 ATM-Mediated DNA Damage Response. J. Nat. Cancer Institute. 2013; 105 : 1355–
504 1364.
505 [13] Weirich G, Klein B, Wöhl T, Engelhardt D, Brauch H (2002) VHL2C Phenotype in a
506 German von Hippel-Lindau Family with Concurrent *VHL* Germline Mutations P81S and
507 L188V. The Jour. of Clin.Endocrinol.& Metabolism . 2002; 87: 5241–5246.
508 [14] Hascoet P, Chesnel F, Jouan F, Goff CL, Couturier A, Darrigrand E, *et al*. The
509 pVHL172 isoform is not a tumor suppressor and up-regulates a subset of pro-
510 tumorigenic genes including TGFB1 and MMP13. 14. Oncotarget/ 2017; Sep 29; 8(44):
511 75989–76002. .
512 [15] Chesnel F, Hascoet P, Gagne JP, Couturier A, Jouan F, Poirier GG, *et al* . The von
513 Hippel-Lindau tumour suppressor gene: uncovering the expression of the pVHL172
514 isoform. Br. J Cancer 2015; 113 : 336–344,
515 [16] Gordan JD., Simon MC. Hypoxia-inducible factors: central regulators of the tumor
516 phenotype. Current Opinion in Genetics & Development. 2007; 17 : 71–77.
517 [17] Gallou C, Chauveau D, Richard S, Joly D, Giraud S, Olschwang S, *et al.* Genotype-
518 phenotype correlation in von Hippel-Lindau families with renal lesions. *Hum Mutat.*
519 2004; 24: 215–224.
520 [18] Gnarra JR, Tory K, Weng Y, Schmidt L, Wei MH, Li H, *et al*. Mutations of the VHL
521 tumour suppressor gene in renal carcinoma. *Nature genetics 1994;* 7: 85–90.
522 [19] Brauch H, Weirich G, Klein B, Rabstein S, Bolt HM, Brüning T. VHL mutations in
523 renal cell cancer: does occupational exposure to trichloroethylene make a difference?
524 Tox.Letters 2004; 151: 301–310
525 [20] Stebbins CE. Structure of the VHL-ElonginC-ElonginB Complex: Implications for VHL
526 Tumor Suppressor Function, Science. 1999; 284 :(455–461.
527 [21] Nguyen HC, Yang H, Fribourgh JL, Wolfe LS, Xiong Y .Insights into Cullin-RING E3
528 Ubiquitin Ligase Recruitment: Structure of the VHL-EloBC-Cul2 Complex. Structure.
529 2015; 23 : 441–449.
530 [22] Minervini G, Pennuto M, Tosatto SCE .The pVHL neglected functions, a tale of
531 hypoxia-dependent and -independent regulations in cancer. Open Biol. 2020; 10
532 :200109.
533 [23] Grosfeld A, Stolze IP, Cockman ME, Pugh CW, Edelmann M, Kessler B, *et al*
534 .Interaction of Hydroxylated Collagen IV with the von Hippel-Lindau Tumor
535 Suppressor.J. Biol. Chem. 2007; 282 : 13264–13269.

[24] Peruzzi B, Athauda G, Bottaro DP. The von Hippel–Lindau tumor suppressor gene product represses oncogenic ᴺL-catenin signaling in renal carcinoma cells, MEDICAL SCIENCES. 2006 ;103 :14531–14536.

[25] Gao S, Liu L, Li Z, Pang Y, Shi J, Zhu F. Seven Novel Genes Related to Cell Proliferation and Migration of VHL-Mutated Pheochromocytoma, Front. Endocrinol. 2021; 12 : 598656.

[26] Chen F, Kishida T, Yao M, Hustad T, Glavac D, Dean M, *et al* .Germline mutations in the von Hippel-Lindau disease tumor suppressor gene: Correlations with phenotype, Human Mutat. 1995; 5 : 66–75.

[27] Ong KR, Woodward ER, Killick P, Lim C, Macdonald F, Maher ER . Genotype-phenotype correlations in von Hippel-Lindau disease, Hum. Mutat. 2007; 28 : 143–149.

[28] Esteban MA, Tran MGB, Harten SK, Hill P, Castellanos MC, Chandra A, *et al* .Regulation of E-cadherin Expression by *VHL* and Hypoxia-Inducible Factor. Cancer Res. 2006; 66: 3567–3575.

[29] Martin B, Chesnel F, Delcros JG, Jouan F, Couturier A, Dugay F, *et al*. Identification of pVHL as a novel substrate for Aurora-A in clear cell renal cell carcinoma (ccRCC). PloS One. 2013; 8 : e67071.

[30] Baux D, Van Goethem C, Ardouin O, Guignard T, Bergougnoux A, Koenig M, *et al*. MobiDetails: online DNA variants interpretation. Eur J Hum Genet. 2021; 29:356–360.

[31] Wiel L, Baakman C, Gilissen D, Veltman JA, Vriend G, Gilissen C. Pathogenicity analysis of genetic variants through aggregation of homologous human protein domains, Human Mutat. 2019; 40 :1030-1038.

Figures legends

Figure 1:

Description of the pedigree of the family which is affected by the P81S mutation.

Pedigree of Family A- ccRCC : clear cell renal cell carcinoma, BC : breast cancer

+ : carrier of the germline c.241C>T, p.Pro81Ser in the vhl gene

- : non carrier of the germline c.241C>T, p.Pro81Ser in the vhl gene

Figure 2: Representation of the $pVHL_{213}$ protein structure

A- Organization of the functional domains and amino acid sequence alignment of $pVHL_{213}$

B- Structural organization of the different domains and amino acid sequence alignment of the $pVHL_{213}$ isoforms. **C**- Pro81 is defining the boundary of secondary structure elements between the beta strands β1 and β2 composing the core of the protein. Several other Proline residues are localized in the extremities of a strand: Pro71 and Pro81 (start and end of beta 1), Pro95 and Pro99 (start and end of beta 3), the pair Pro102 and Pro103 (start of beta 4) and Pro146 and Pro154 (start and end of beta 7).

Figure 3 : Characterization of the stable cell lines expressing the $pVHL_{213}$-P81S

A- pVHL expression in 786-O, 786-O-$pVHL_{172}$ and 786-O-$pVHL_{213}$ and 786-O-$pVHL_{213}$ P81S cells (different clones : E1, E6 and C7) assessed by immunoblotting with the indicated antibodies VHL (JD-1956-[15]) and GAPDH .**B-** Stability of pVHL was assessed in the different 786-O-$pVHL_{213}$ and 786-O-$pVHL_{213}$ P81S cell lines after treatment with cycloheximide for 3 and 7 hours. HIF-2α protein expression level was also evaluated by immunoblotting in the three cell lines 786-O, 786-O-$pVHL_{213}$ and 786-O-$pVHL_{213}$ P81S. Immunodetection of Cyclin D1 was performed as a control of the efficiency of treatment with CHX. GAPDH was used as a loading control. **C**- The histogram shows the quantification of the amount of pVHL (mean ±SEM; n=3) in 786-O-$pVHL_{213}$ and 786-O-$pVHL_{213}$ P81S.

D- The histogram illustrates the amount of HIF2-α detected in the three 786-O, 786-O-$pVHL_{213}$ and 786-O-$pVHL_{213}$ P81S cell line before (0) or after treatment with CHX for 4 or 7 hours. The results are expressed as the mean ±SEM of three independent experiments (** *p value :0.00173)* and (**p=,0.04156)*. **E-** Effect of Hypoxia induced by incubation of the cells with $CoCl_2$ during 19 hours on the amount of HIF2-α in the absence (or presence of $pVHL_{213}$ or $pVHL_{213}$ P81S. HIF2-α, VHL (and GAPDH as a loading control) were detected by Western Blot **F**- Quantification of the immunodetected amount of HIF2-α from five independent experiments (**t-test, p=0.02616 ; * t-test, p=0.004998 ; *ns* Non significant).

Figure 4: pVHL$_{213}$-P81S is part of the E3 ligase complex

A- 786-O, 786-O-pVHL$_{213}$ and 786-O-pVHL$_{213}$ P81S cell lines were cultivated in the presence of MG132 for 2 or 5 hours. The amounts of VHL, Cul2 and HIF2-α were estimated following their detection by immunoblotting. GAPDH was used as a loading control to normalize the level of each protein **B-** Flag immunoprecipitation was performed with total protein extracts from the 3 cell lines and for each time of MG132 incubation. The proteins VHL, HIF2-α and Cul2 were then immunoblotted in the bound fractions. **C-** The ratio CUL2/VHL and HIF2-□/VHL was calculated from five independent experiments. The histogram shows the quantification of the amount of CUL2/VHL (mean ±SEM; n=5) and HIF2-α/VHL in 786-O-pVHL$_{213}$ and 786-O-pVHL$_{213}$ P81S. Quantification of the immunodetected amount of HIF2-α /VHL from five independent experiments *(**t-test, p=0.0041 ; * t-test, p=0. 0313* ; *ns* Non significant). D- Functional HRE-dependent reporter assays were performed in 786-O cells (*i.e.* VHL negative cells that constitutively accumulate HIF-2α in normoxia. The results are expressed as relative Firefly luciferase activity with Renilla luciferase as an internal control. 1unit denotes the basal activity of endogenous HIF-2α using the HRE-luciferase reporter plasmid. The abilities of pVHL$_{213}$ and pVHL$_{213}$-P81S to downregulate Firefly luciferase activity (related to HIF activity) were compared.

Figure 5: Expression of pVHL$_{213}$-P81S promotes cell migration.

A-The 786-O, 786-O-pVHL$_{213}$ and 786-O-pVHL$_{213}$-P81S cell were seeded in culture inserts. Analysis of cell migration by wound healing assay was then carried out with images taken every hour for 16 hours. **B-** Results were expressed as the percentage of wound closure at the indicated time points. The average corresponded to of 3 wells per cell line from 6 independent experiments is shown. **C-**Time needed for 50% closure was estimated for each cell line **(**mean ±SEM; 786-O and 786-O-pVHL$_{213}$ (n=7 *p-value 0.0006333 - t-test*) 786-O pVHL$_{213}$ -and 786-O-pVHL$_{213}$-P81S (n=7 *p-value 0.0003016 - t-test*)7 86-O and 786-O-pVHL$_{213}$-P81S (n=6 *p-value : p 0,01342 - t test*).

Figure 6: Tumorigenic effect of pVHL$_{213}$-P81S in 786-O cells

A-Morphology of 786-O, 786-O-pVHL$_{213}$ and 786-O-pVHL$_{213}$-P81S spheroids. Spheroid aspect was obtained after 48hours of incubation of cells on poly-Hema coated wells. Spheroids were imaged under Leica microscope. Scale bars: 100 µm. **B-** The spheroids were collected 48 hours post seeding and pVHLs expression was evaluated by western blot. GAPDH was used a loading control. **C-**The spheroids corresponding to the 3 different cell lines were loaded into Matrigel. The spheroid morphology was recorded during 24 hours. The picture showed the spheroids after 24 hours of incubation. **D** Actin staining, analyzed after Rhodamin-phalloidin

627 incubation of 786-O cells (upper panel), 786-O pVHL$_{213}$ (middle panel) and 786-O pVHL$_{213}$-
628 P81S cells (lower panel). (scale bar: 25µm)
629

Additional Information

Acknowledgements

We thank the IGDR for all facilities. We would like to acknowledge S. Dreano (IGDR) for his contribution in plasmids sequencing. We acknowledge the ImPAcCell and MRic microscopy platforms at the SFR BIOSIT (CNRS UMS3480 Rennes). We thank the LNCC for financial support of this study. We thank L. Schmitt for its contribution to the revision experiments.

Authors contribution

Conceived and designed the experiments: FC YAB. Performed the experiments: FC ,AA AC EJ ML XLG .Analyzed the data : FC XLG BG YAB. Contributed reagents/materials/analysis data from patients: CA, BG. Wrote the paper: YAB.

Ethics approval and consent to participate:

No applicable

Competing Interests

No applicable

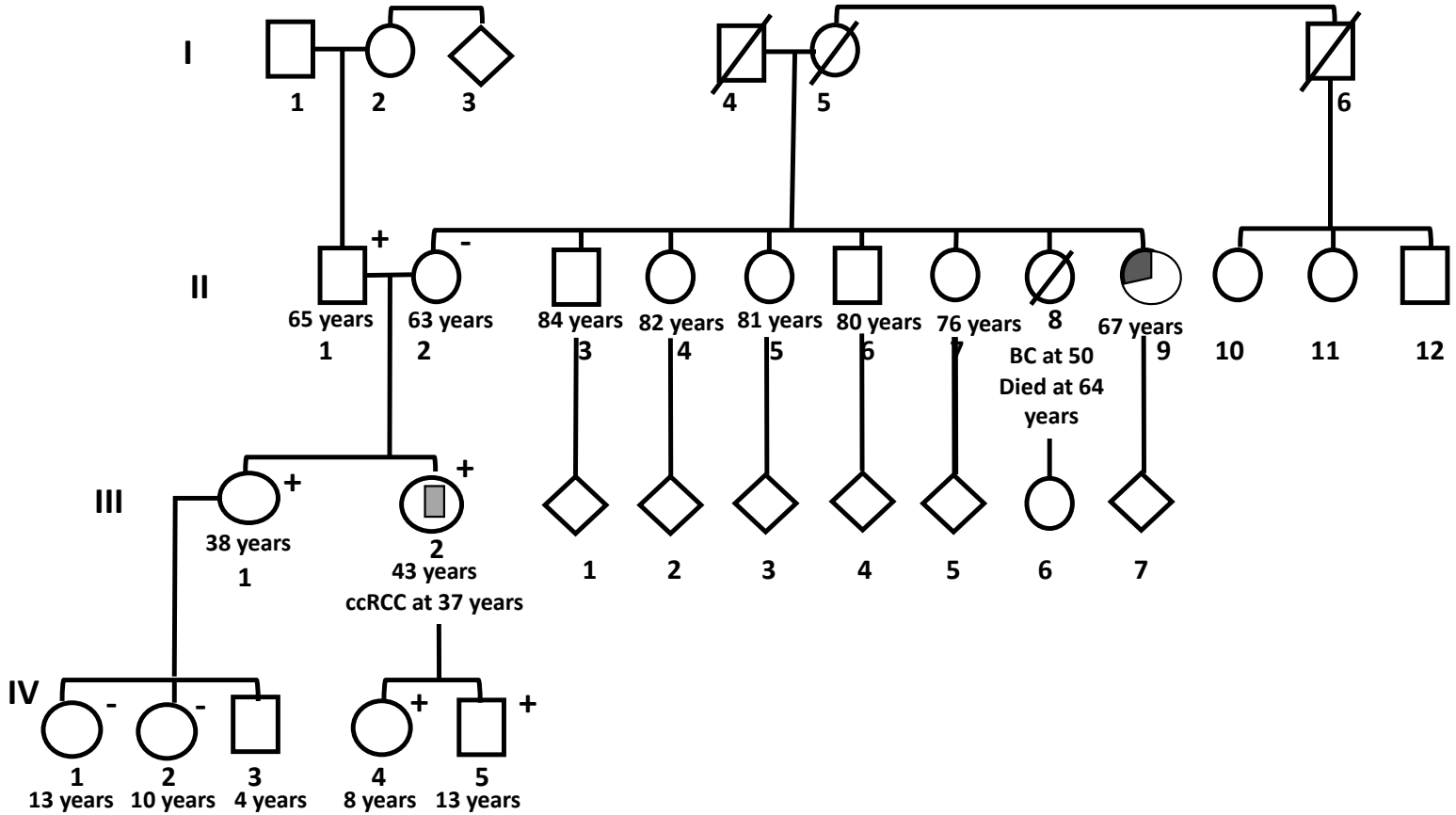

Chesnel et al 2022, Figure 1

A

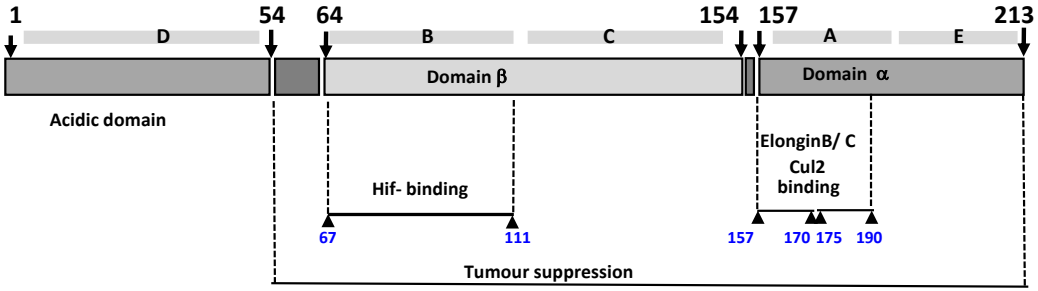

B

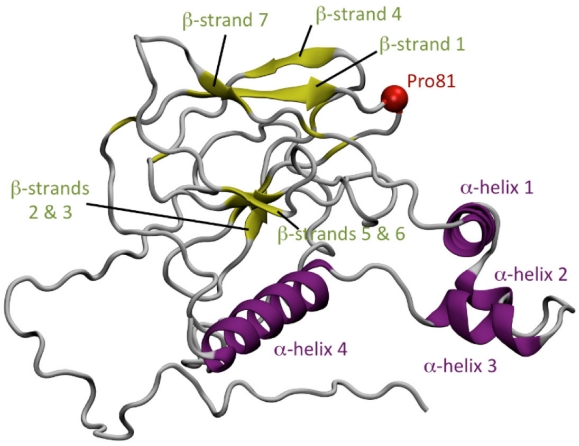

C

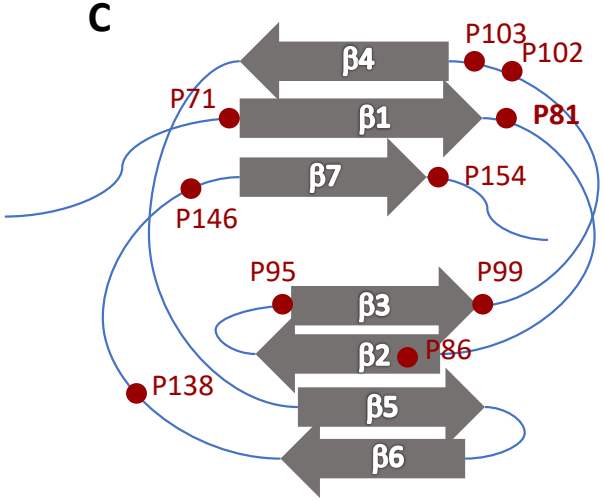

Chesnel et al 2022, Figure 2A,B,C

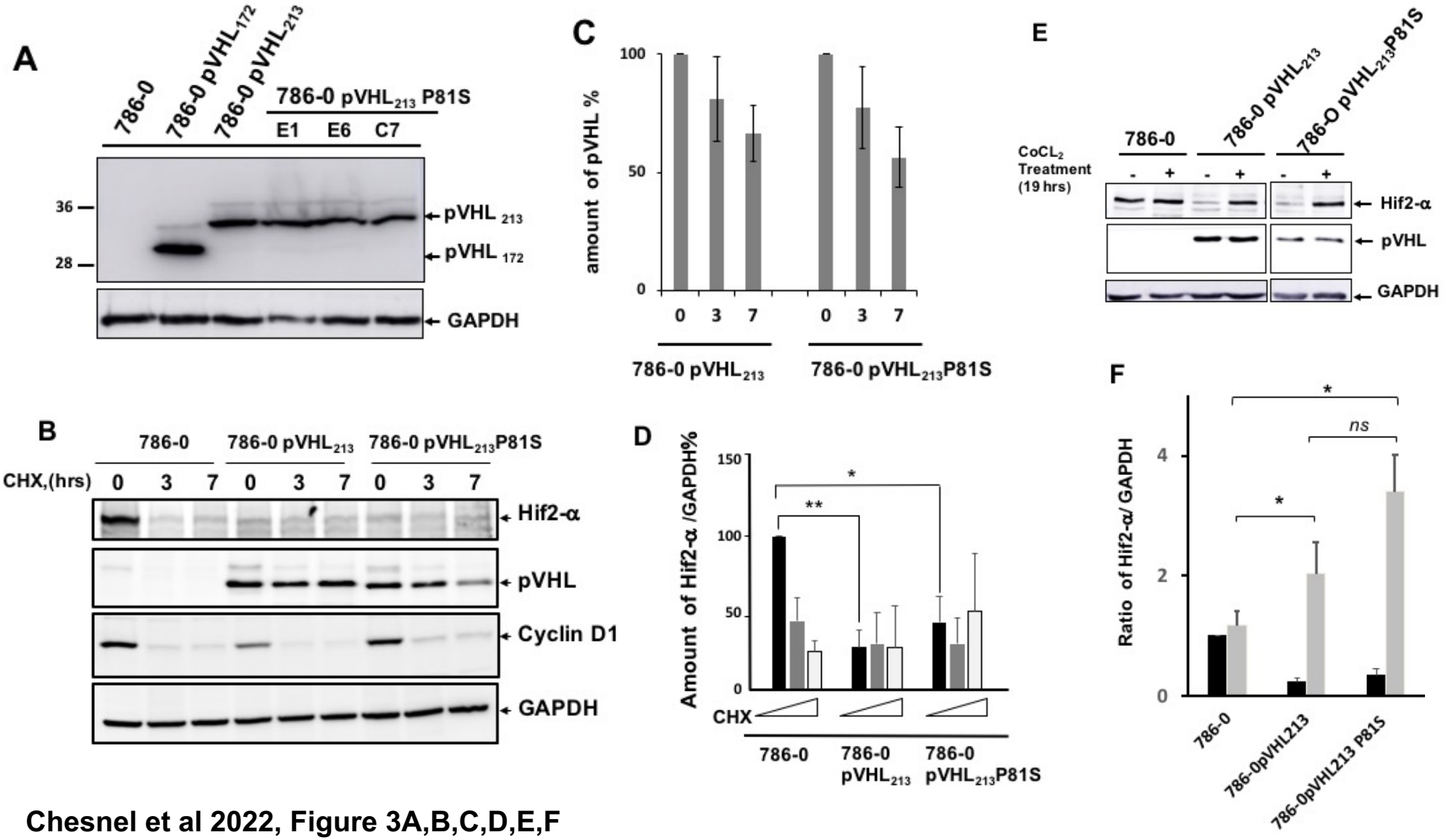

Chesnel et al 2022, Figure 3A,B,C,D,E,F

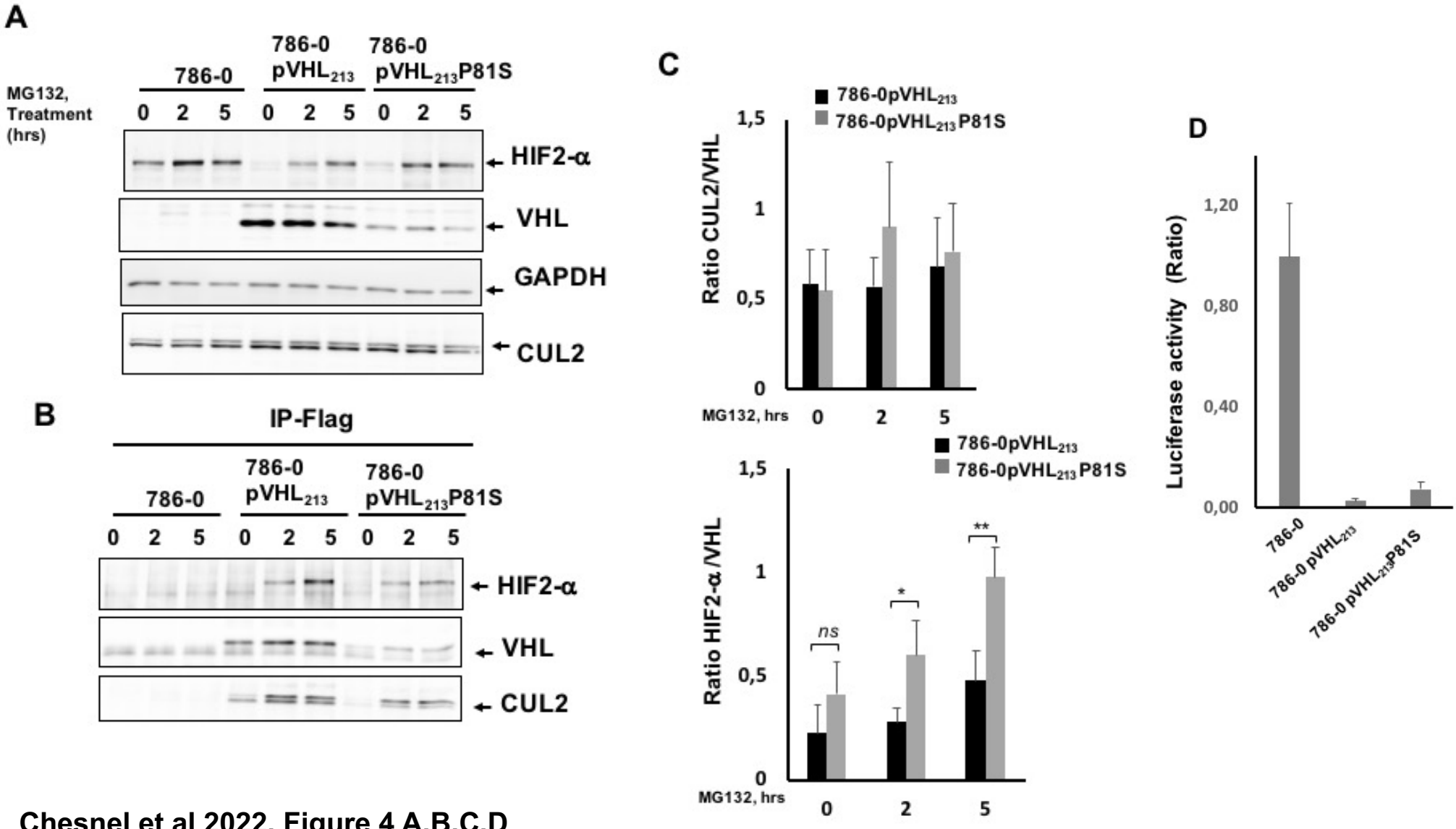

Chesnel et al 2022, Figure 4 A,B,C,D

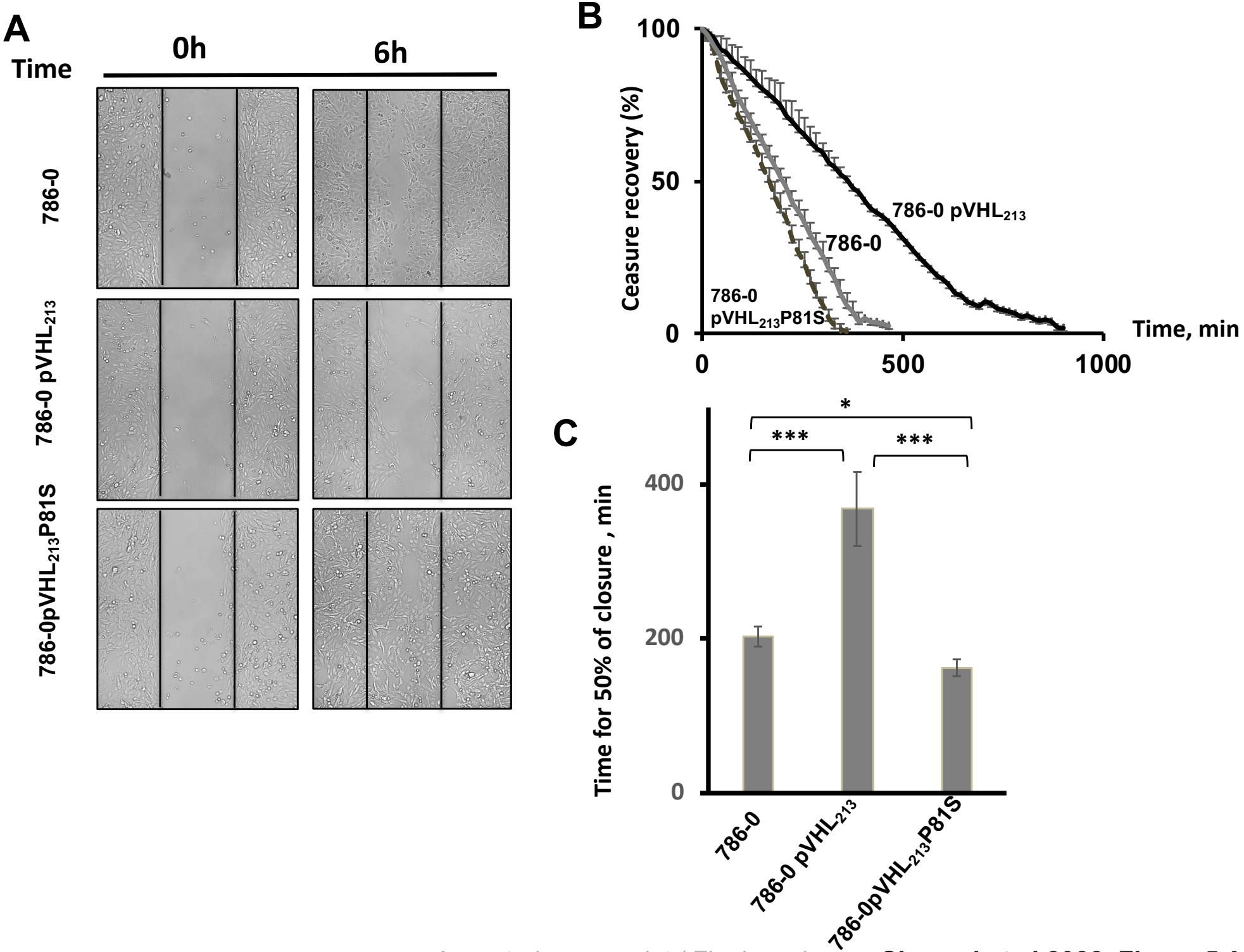

Chesnel et al 2022, Figure 5 A,B,C

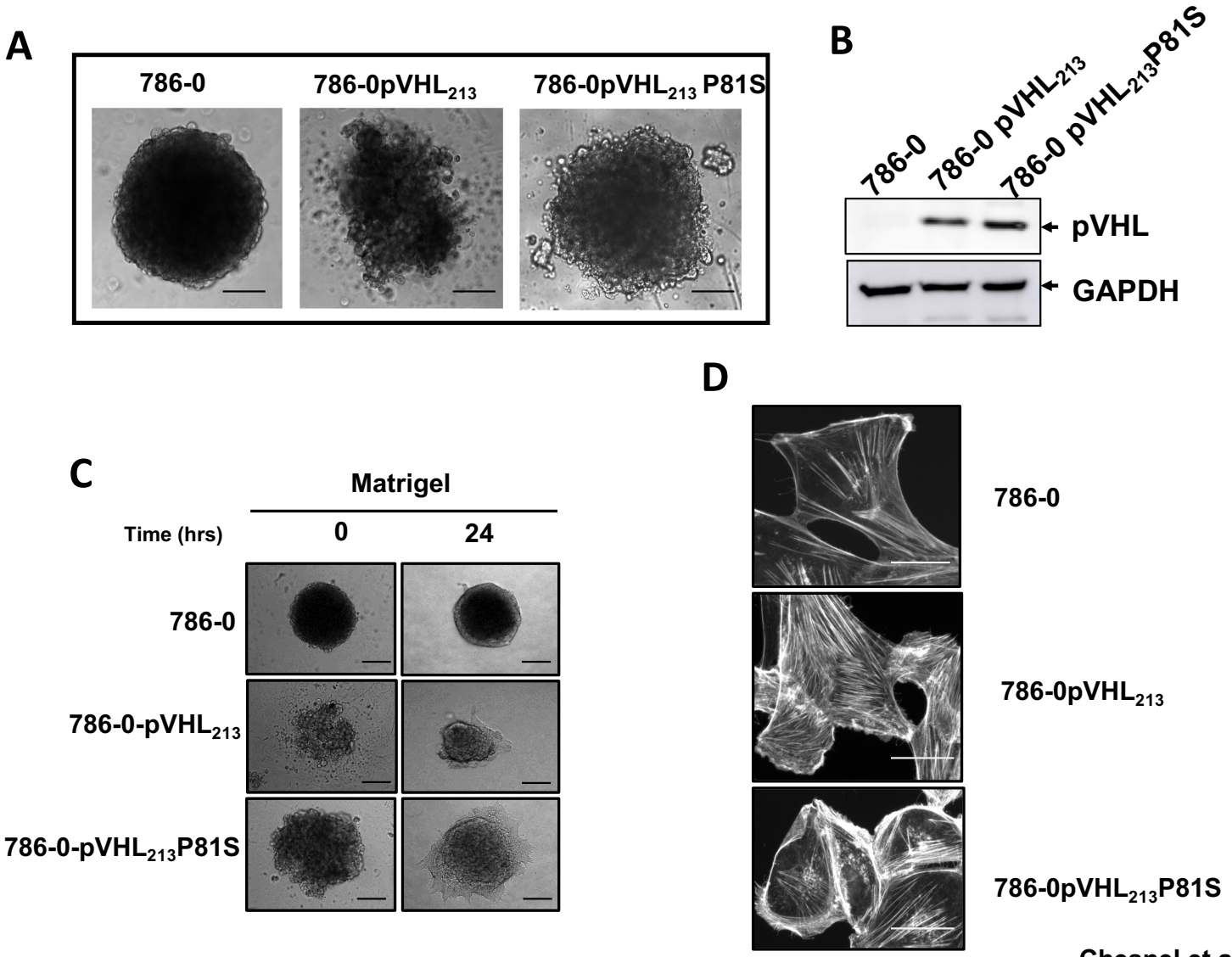

Chesnel et al 2022, Figure 6 A,B,C,D

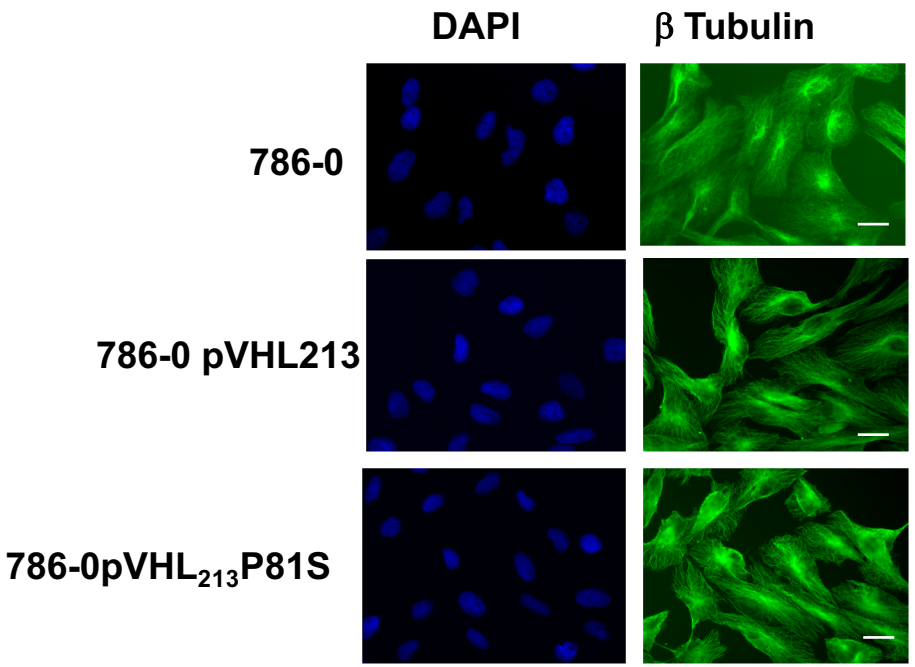

Chesnel et al, Supp Figure 1

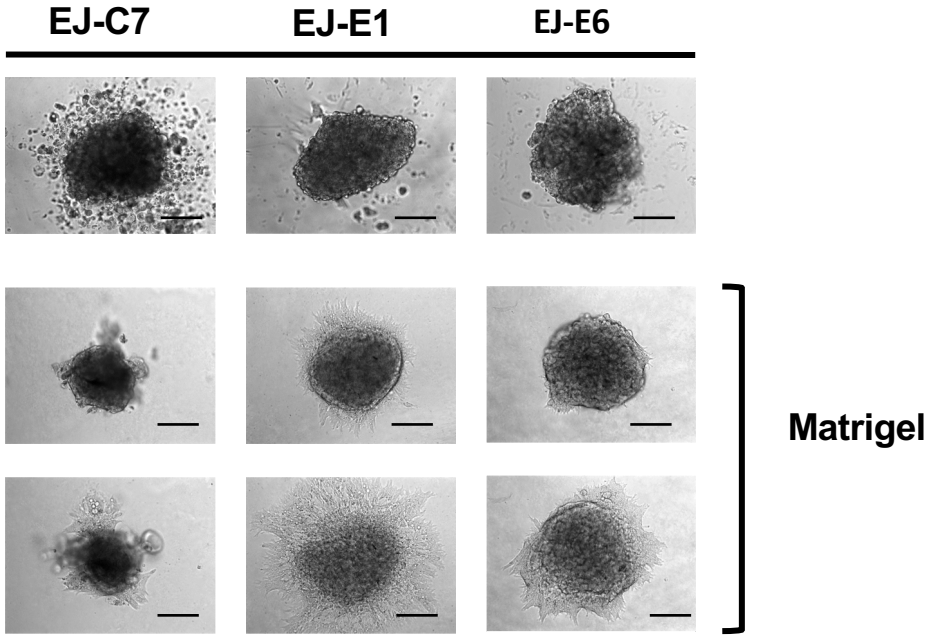

Chesnel et al ,Supp Figure 2

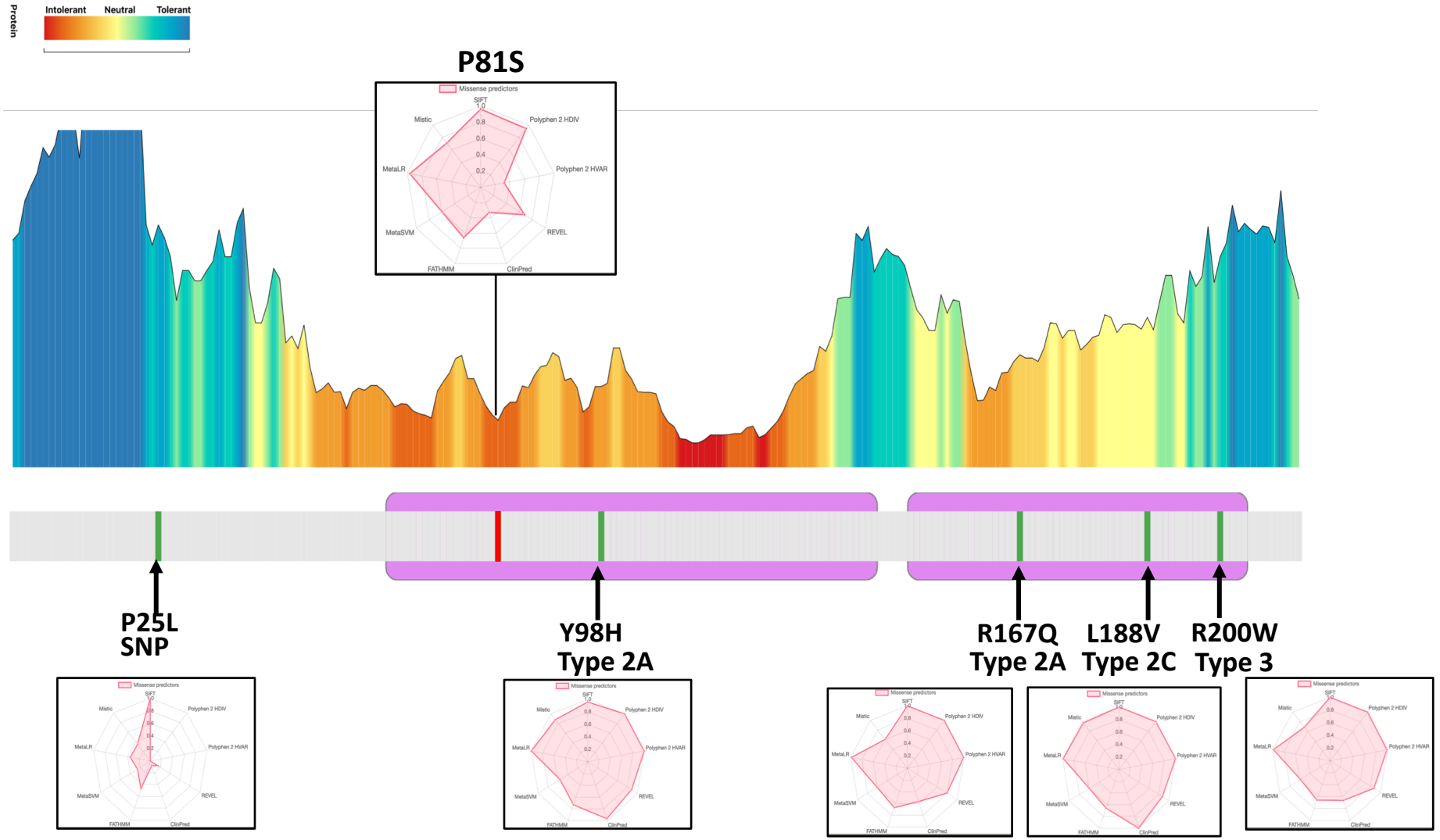

Chesnel et al ,Supp Figure 3

Supplementary figures

Figure S1: Morphological analysis of the 786-O- pVHL$_{1213}$P81S - cell line.

Tubulin staining, analyzed by immunofluorescence using an anti-β-tubulin antibody in 786-O (upper panels), 786-O-pVHL$_{213}$ (middle panels) and 786-O-pVHL$_{213}$-P81S cells (lower panels). (scale bar: 25µm).

Figure S2:

Analysis of the spheroids resulting from the seeding of different clones 786-O-pVHL$_{213}$-P81S after loading on matrigel for 24 hours. Scale bars: 100 µm

Figure S3:

MetaDome analysis for mutation P81S in the gene vhl. P25L was described as non pathogenic Y98H, R167Q, L118V and R200W as pahtogneic (Hoffman, 2001)(Tomasic *et al*, 2013)(Knauth *et al*, 2009)(Lee *et al*, 2009)